

Transition Metal Complexes with Sterically Demanding Ligands. 2.¹ Meisenheimer Complex Formation and Deprotonation Reactions of a Sterically Demanding Aromatic Diimine[†]

Stefan Nüchel and Peter Burger*

Anorganisch-chemisches Institut der Universität Zürich, Winterthurerstrasse 190,
CH-8057 Zürich, Switzerland

Received February 1, 2000

The synthesis of the novel diimine **1** is described, and its low/absent propensity for the complexation of group 9 transition metals (Co, Rh, Ir) is rationalized by a potentially difficult C–H activation step required for terdentate coordination. To overcome this problem, deprotonation of this unique C–H bond in **1** with a variety of bases was attempted. The unexpected outcome of these reactions, including the formation of the Meisenheimer complex **3** by addition of butyllithium, is reported. In addition, the formation of the double-addition product **4** through reaction with *t*-BuLi is described. Deprotonation at the diimine methyl group with the hard base lithium dimethylamide gives the corresponding diketiminate **5**. The structures of the novel compounds **1** and **3**–**5** were unambiguously confirmed by X-ray crystal structure analyses.

Introduction

Sterically demanding diimine and amido nitrogen donor ligands have recently attained considerable interest in transition metal chemistry. This is best exemplified through the fascinating middle to late transition metal olefin polymerization catalysts developed by Brookhart's and Gibson's groups^{2–5} and Cummins⁶ exciting results on dinitrogen cleavage at room temperature with molybdenum amido complexes. Problems frequently encountered in the syntheses of these systems, however, are large barriers for the attachment of the bulky nitrogen donors to the metal center. In most cases this has been solved by (a) using metal complexes with labile groups as starting materials or (b) if applicable, using more reactive anionic ligands, such as alkali metal amides. Recently, we have explored this area and reported a labile Pd triflate complex using the methodology described in (a).¹ Herein, we report on the unexpected synthetic and structural results we encountered when we attempted to convert the *neutral* sterically demanding diimine donor ligand **1** into its more reactive anionic congeners.

Results and Discussion

The synthesis of the novel diimine donor **1** is straightforward from the aromatic ketone and 2,6-diisopropyl-

aniline and follows a route very recently reported for the corresponding terdentate pyridine, diimine nitrogen analogue **1a** (Scheme 1).^{2,5} Compound **1a** has been successfully used as a ligand in highly active iron- and cobalt-based ethylene polymerization catalysts, which were prepared from readily available starting materials such as CoCl₂·6H₂O.^{2,5}

However, in contrast to the results observed for ligand **1a**^{2,5} and also derivatives of it with different diimine N-substituents,⁷ we were not able to obtain detectable amounts of metal complexes containing ligand **1** from Co(II) or other Rh(I, III) and Ir(I, III) starting materials even under very harsh reaction conditions. Since this apparent difference between ligands **1** and **1a** was likely due to the requirement of a *potentially* difficult C–H activation step at carbon atom C2 in **1** to enable terdentate coordination to the metal center, we have considered deprotonation of this unique C–H unit with strong bases, such as *n*-BuLi, in an attempt to obtain **2** (Scheme 1). It should be noted that a similar strategy has been developed and applied with success for the synthesis of complexes with the tweezer (terdentate) amine ligand 1,3-(CH₂NMe₂)₂C₆H₄ by van Koten et al.⁸ On the basis of their results, we anticipated that deprotonation might proceed regioselectively at the C2 position due to the neighboring group effect of the diimine donors (Scheme 1).

Upon addition of an equimolar amount of *n*-BuLi/TMEDA (1:1) to **1** in pentane, an immediate color change from pale yellow to ink-blue was observed (Scheme 1). From this mixture, the very air-sensitive,

[†] Dedicated to H.-H. Brintzinger on the occasion of his 65th birthday.

(1) Burger, P.; Baumeister, J. M. *J. Organomet. Chem.* **1999**, *575*, 214.

(2) Britovsek, G. J. P.; Gibson, V. C.; Kimberley, B. S.; Maddox, P. J.; McTavish, S. J.; Solan, G. A.; White, A. J. P.; Williams, D. J. *Chem. Commun.* **1998**, 849.

(3) Johnson, L. K.; Killian, C. M.; Brookhart, M. *J. Am. Chem. Soc.* **1995**, *117*, 6414.

(4) Johnson, L. K.; Mecking, S.; Brookhart, M. *J. Am. Chem. Soc.* **1996**, *118*, 267.

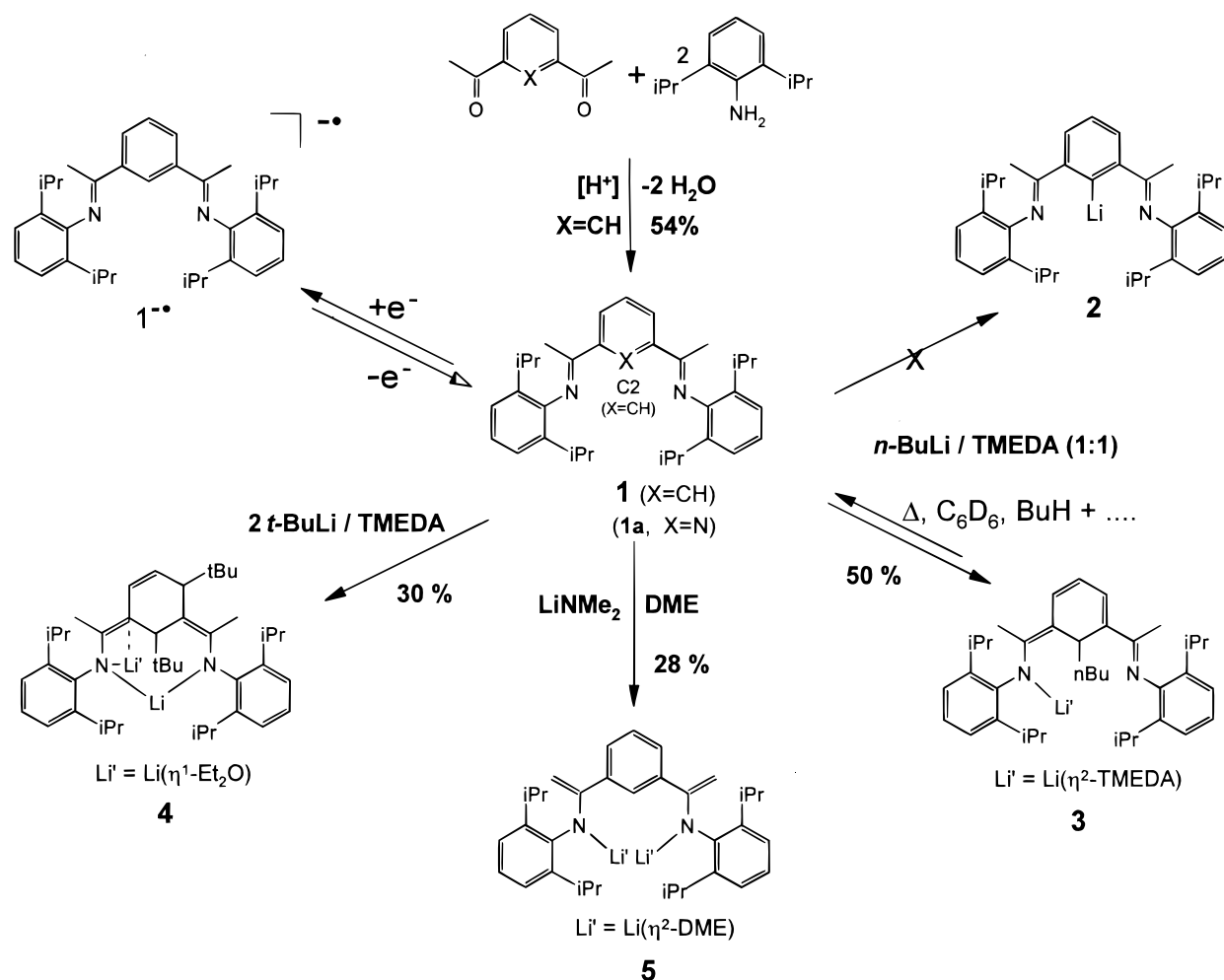
(5) Small, B. L.; Brookhart, M.; Bennett, A. M. A. *J. Am. Chem. Soc.* **1998**, *120*, 4049.

(6) LaPlaza, C. E.; Cummins, C. C. *Science* **1995**, *268*, 861.

(7) Aleya, E. C.; Merrell, P. H. *Synth. React. Inorg. Met.-Org. Chem.* **1974**, *4*, 535. Haarman, H. F.; Bregman, F. R.; Ernsting, J.-M.; Veldman, N.; Spek, A. L.; Vrieze, K. *Organometallics* **1997**, *16*, 54.

(8) Rietveld, M. H. P.; Grove, D. M.; van Koten, G. *New J. Chem.* **1997**, *21*, 751 and literature cited therein.

Scheme 1



red crystalline material **3** could be isolated in 50% yield. The complex 1H and ^{13}C NMR spectra of **3**, and in particular its unexpected red color, immediately hinted toward a reaction scheme far more complex than a simple deprotonation reaction. This was further substantiated by the complex 1H NMR spectrum recorded for the hydrolysis product(s) of **3**, which did not display the anticipated signals for **1**. The X-ray crystal structure analysis of the red crystalline material **3** unambiguously confirmed that, rather than acting solely as a base, *n*-butyllithium had added to the central aromatic core to give the Meisenheimer butyllithium adduct **3** presented in Figure 1. Details of the data collection are summarized in Table 1; selected distances and angles are given in Table 2.

For comparison of the bonding situation in **3** and further compounds described herein, we have also performed an X-ray crystal structure analysis of the diimine starting material **1**. The molecular structure of **1** is presented in Figure 2; selected distances and angles are compiled in Table 3 and details of the data collection in Table 1.

By comparison of the geometrical data observed in the X-ray crystal structures of **1** and **3** shown in Chart 1, the prominent resonance structure of **3** (right-hand side) manifested itself (distances shown). The latter is reminiscent of a merocyanine, which readily explains its observed blue color (low-energy absorption).

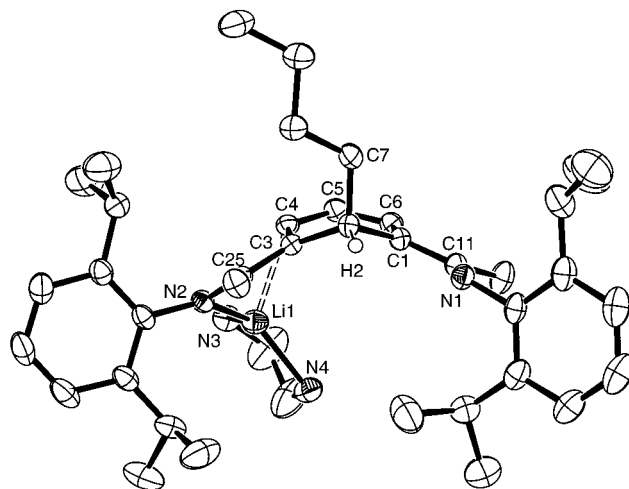


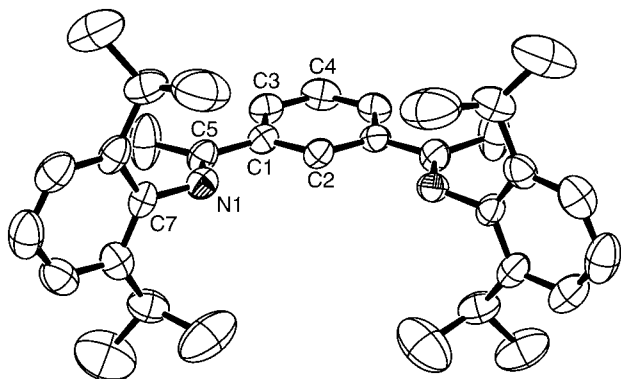
Figure 1. Ortep plot of **3** shown at the 50% probability level. The methyl groups of the TMEDA ligand are omitted for clarity. The hydrogen atom presented, H2, was localized in the difference Fourier map.

While Meisenheimer complexes of arenes substituted with nitro or triflate substituents are well-known,⁹ it should be emphasized that to the best of our knowledge there are no isolated examples of such an anionic σ -complex with aldehyde/ketone or imine groups. This

(9) Terrier, F. *Chem. Rev.* **1982**, 82, 77; M. J. Strauss, *Acc. Chem. Res.* **1974**, 7, 181.

Table 1. Crystal and Data Collection Parameters for 1, 3, 4·0.5Et₂O, and 5

	1	3	4·0.5Et ₂ O	5
formula	C ₃₄ H ₄₄ N ₂	C ₄₄ H ₆₉ LiN ₄	C ₄₈ H ₇₇ Li ₂ N ₂ O _{1.5}	C ₄₂ H ₆₂ Li ₂ N ₂ O ₄
fw	480.7	661.0	720.0	672.8
color, habit	pale yellow, cube	red, rect parallelepiped	yellow, rect parallelepiped	pale yellow, plate
cryst size (mm)	0.2 × 0.2 × 0.2	0.2 × 0.3 × 0.2	0.1 × 0.2 × 0.3	0.05 × 0.2 × 0.2
cryst syst	orthorhombic	triclinic	monoclinic	monoclinic
space group	<i>Fdd2</i> (No. 43)	<i>P1</i> (No. 2)	<i>P2₁/c</i> (No. 14)	<i>P2₁/a</i> (No. 15)
<i>a</i> (Å)	16.319(3)	9.163(1)	12.979(1)	14.356(1)
<i>b</i> (Å)	49.650(10)	10.253(1)	15.703(1)	14.888(1)
<i>c</i> (Å)	7.487(1)	23.038(3)	22.942(2)	19.760(2)
α (deg)		88.71(1)		
β (deg)		80.04(1)	94.61(1)	99.00(1)
γ (deg)		81.62(1)		
<i>V</i> (Å ³)	6066.3(2)	2109.0(4)	4660.7(6)	4171.4(6)
<i>Z</i>	8	2	4	4
calcd density (Mg/m ³)	1.05	1.04	1.02	1.07
temp (K)	183	193	183	193
λ(Mo Kα) (Å)	0.710 73	0.710 73	0.710 73	0.710 73
scan type	image plate	image plate	image plate	image plate
2θ range (deg)	5–48	6–52	4 ? 48	6–52
no. of rflns measd: total, unique	10 060, 2273	20 696, 6625	34 044, 7236	21 390, 3771
no. of params	169	479	517	331
R1(<i>F</i> ² > 2σ(<i>F</i> ²))	0.0499	0.0557	0.0429	0.0632
wR2(<i>F</i> ² > 2σ(<i>F</i> ²))	0.0909	0.1517	0.0687	0.1629
GOF, <i>S</i>	0.992	1.034	0.65	1.068
resid e density (e/Å ³)	0.15, −0.15	0.26, −0.23	0.39, −0.30	0.20, −0.16

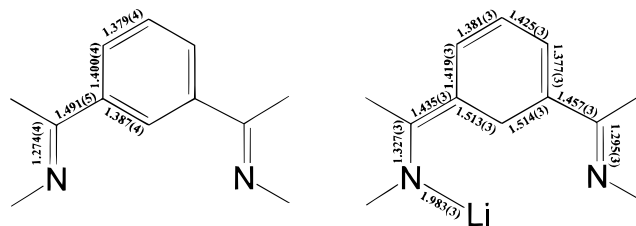
**Figure 2.** Ortep plot of the diimine **1** (50% probability level). The molecule is located on a crystallographic C₂ axis passing through atoms C2 and C4.**Table 2. Selected Distances (Å) and Angles (deg) for 3**

C1–C2	1.514(3)	C2–C3	1.513(3)
C3–C4	1.419(3)	C4–C5	1.381(3)
C5–C6	1.425(3)	C1–C6	1.377(3)
C2–C7	1.555(3)	C1–C11	1.457(3)
C11–N1	1.295(3)	C3–C25	1.435(3)
C25–N2	1.327(3)	Li1–N2	1.983(5)
Li1–N3	2.080(5)	Li1–N4	2.139(5)
Li1–C4	2.409(5)		
C3–C2–C1	107.7(2)	C3–C2–C7	113.4(2)
C1–C2–C7	107.9(2)		

is readily explained by the fact that nucleophilic attack occurs preferentially at the C=O or C=N sites rather than the aromatic core. In this regard it is interesting to note that we could not detect any product arising from nucleophilic attack at the carbon atom of the imine group, which might be attributed to steric shielding of the 2,6-diisopropylphenyl groups of the diimine moiety. The outcome of this reaction can be rationalized by considering the strongly electron-withdrawing ketimine groups, which lead to a suitably electron-deficient aromatic system in which nucleophilic attack of the butyl anion rather than deprotonation at carbon atom C2 is preferred. The cyclic voltammogram of **1** in THF

Table 3. Selected Distances (Å) and Angles (deg) for 1

C1–C2	1.387(4)	C1–C3	1.400(4)
C3–C4	1.379(4)	C1–C5	1.491(5)
C5–C6	1.515(5)	N5–N1	1.274(4)
N1–C7	1.433(4)		
C6–C5–C1	117.9(3)	C6–C5–N1	124.3(4)
C1–C5–N1	117.8(4)	C5–N1–C7	121.7(4)
C8–C7–N1–C5			91.2
C1–C5–N1–C7			16.7
N1–C5–C1–C2			2.7

Chart 1

presented in Figure 3 displays a reversible one-electron reduction wave at −2440 mV with $\Delta E_p = 70$ mV and provides further support for this view. This was further substantiated through preliminary results of the independent chemical 1 e reduction of **1** with Li in 1,2-dimethoxyethane (DME) similar to Birch reduction conditions.¹⁰

In these experiments, dark blue solutions quite similar to those observed in the butyllithium addition to **1** (Scheme 1) were obtained. We have tentatively assigned this blue species to the monoradical anion **1**^{•−}; attempts to isolate and fully characterize this species have so far been thwarted by the fact that in a

(10) Birch, A. J. *Pure Appl. Chem.* **1996**, *68*, 553.(11) Further support for the structure of species **1**^{•−} was provided from a time-dependent open-shell UHF calculation (URPA) of the fully geometry optimized model compound 1,3-(−CH=NH)₂C₆H₄^{•−} (TZVP basis applied), from which the three lowest transitions at 1203 (0.04), 578 (0.08), and 438 (0.027) nm were calculated (oscillator strengths in parentheses). The observed blue color of this species can be explained

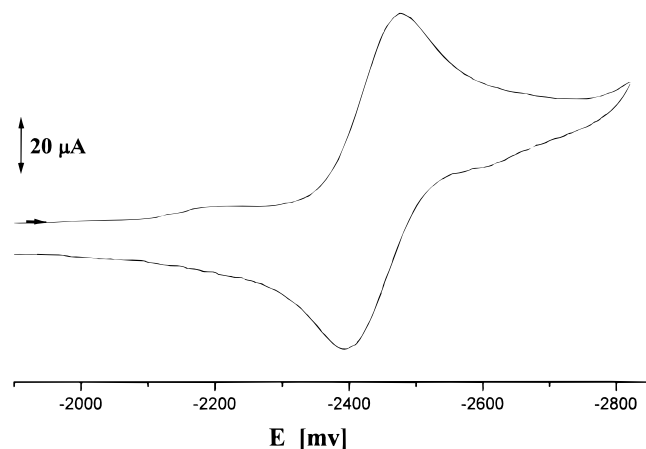


Figure 3. Cyclic voltammogram of **1** in THF referenced to the $\text{Cp}_2\text{Fe}/\text{Cp}_2\text{Fe}^+$ couple. Conditions: glassy-carbon working electrode (o.d. 1.2 mm); Ag/Ag^+ reference electrode; $[\mathbf{1}] = 10^{-3}$ M, $[\text{NBu}_4\text{PF}_6] = 3 \times 10^{-1}$ M.

slower reaction, further conversion to the final product, the deprotonated dilithium diketiminate **5** (vide infra), occurs within a short period of time at room temperature. Nevertheless, this circumstantial evidence points to the monoradical anion $\mathbf{1}^{\cdot-}$ as a one-electron reductive transient in the reaction of **1** with BuLi. This implies an SET-type mechanism for the addition of butyllithium to **1** with the one-electron transfer preceding the C–C bond formation step. Since DFT calculations on the anionic model compound for **3**, i.e., 1,3,2-(–CH=NH)₂–(Bu)C₆H₄[–], suggested a substantial accumulation of negative charge at the α-CH₂ carbon atom (–0.35 e, Hirshfeld charge) of the butyl group in the model system,¹² we were intrigued by the idea that the desired deprotonated product **2** could still be available from **3** upon thermolysis. Indeed, a change of the initial blue solution of **3** to red was noticed in the course of the thermolysis performed in C₆D₆. ¹H NMR and GC/MS studies clearly established that the butyl addition to the aromatic ring was reversible, which was evidenced through the formation of butane and butane-*d*. However, rather than the expected lithiated product **2**, the protio compound **1** was recovered in nearly quantitative yield in these reactions. The ²H NMR spectrum of the final product revealed incorporation of deuterium into the imine methyl group, which is presumed to originate from the deuterated solvent. So far, we have not been able to identify the final lithium-containing product(s); thermolysis studies of other lithium organyls, however, allow us to suggest lithium hydride as a potential candidate.¹³ To prevent the formation of the Meisenheimer adduct, we have turned to the less nucleophilic and stronger base *tert*-butyllithium. Again, quite unexpectedly, we have isolated and crystallographically characterized the yellow-orange compound **4** in 30% yield (Scheme 1). This compound is formed through double

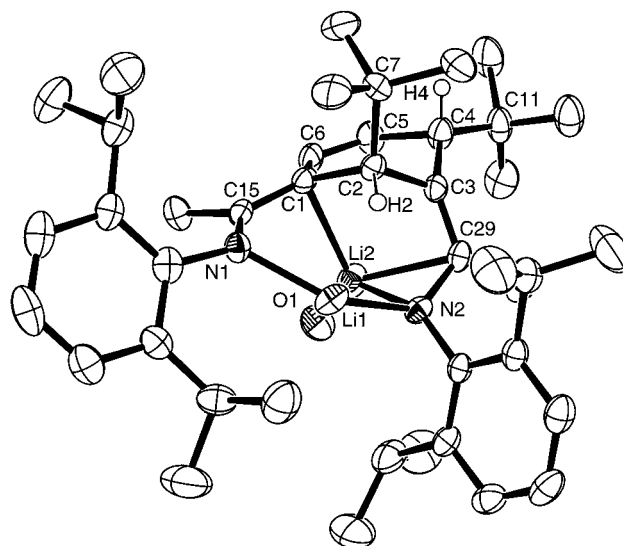


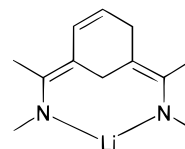
Figure 4. Ortep plot (50% probability level) of **4**·0.5Et₂O. The ethyl groups of the coordinated ether and the second ether molecule (not coordinated) are omitted for clarity.

Table 4. Selected Distances (Å) and Angles (deg) for **4**·0.5Et₂O

C1–C2	1.527(4)	C2–C3	1.548(4)
C3–C4	1.543(4)	C4–C5	1.529(4)
C5–C6	1.362(4)	C1–C6	1.446(4)
C1–C15	1.406(4)	C15–N1	1.358(3)
C3–C29	1.363(4)	C29–N2	1.438(3)
C2–C7	1.594(4)	C4–C11	1.558(4)
C17–N1	1.416(3)	C31–N2	1.430(3)
Li1–N1	1.934(5)	Li1–N2	1.964(5)
Li2–N2	2.081(6)	Li2–C1	2.326(6)
Li2–C29	2.259(6)	Li2–O1	1.945(6)
C1–C2–C3	107.0(2)	C1–C2–C7	114.0(2)
C3–C2–C7	117.0(2)	C29–C3–C2	116.7(2)
C29–C3–C4	131.4(3)	C2–C3–C4	108.9(2)
C5–C4–C3	104.2(2)	C5–C4–C11	113.4(3)
C3–C4–C11	126.4(3)	C6–C5–C4	123.5(3)
C1–C6–C5	123.9(3)		

addition of the *t*-Bu group in the 2- and 4-positions to the central aromatic core of **1**, which is best illustrated through the molecular structure of **4** shown in Figure 4. Details of the data collection are summarized in Table 1; selected geometrical data are given in Table 4.

Two lithium centers with different coordination modes are observed in the X-ray crystal structures with lithium atom Li1 being two-coordinate. It is noteworthy that this structure is apparently also maintained in solution, as evidenced by two distinctly separated resonances in the ⁷Li NMR at δ –1.77 and 1.60, respectively. On the basis of the distances and angles in the molecular structure of **4**, in particular, the lengths of the exocyclic bonds in the former central aromatic ring, i.e., C1–C15 = 1.406(4) Å and C3–C29 = 1.363(4) Å and, in addition, the C–N bonds of the imine unit C29–N2 = 1.438(3) Å and C15–N1 = 1.358(3) Å, this compound is best described with a bis(enamido) structure:



Further support for this view is provided through the rather short lithium nitrogen distances (Li–N1 =

with the transition at 578 nm. The computations were performed with the Turbomole program package with additions recently made for open-shell systems: Bauernschmitt, R.; Häser, M.; Treutler, O.; Ahlrichs, R. *Chem. Phys. Lett.* **1997**, 64, 573.

(12) The calculations were performed with, Delley's DMOL DFT program package using the Becke-Perdew86 functional and dnp-basis sets: Delley, B. *J. Chem. Phys.* **1990**, 92, 508. Becke, A. D. *Phys. Rev. A* **1988**, 38, 3098. Perdew, J. P. *Phys. Rev. B* **1986**, 33, 8822.

(13) Sapsee, A.-M.; Schleyer, P. v. R., Eds. *Lithium Chemistry*; Wiley-Interscience: New York, Chichester, Brisbane, Toronto, Singapore, 1995.

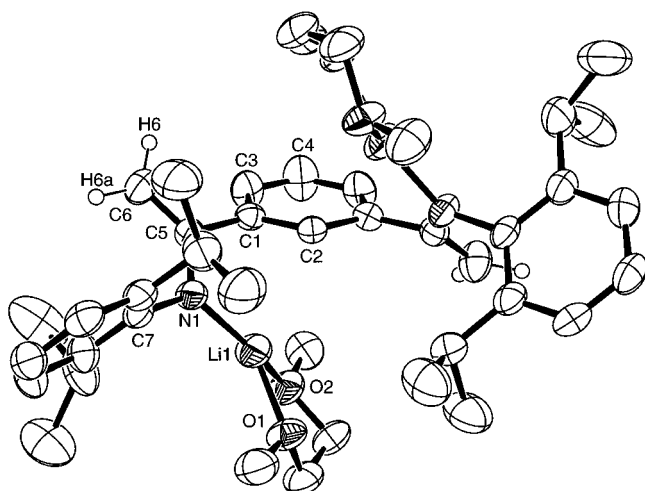


Figure 5. Ortep plot of **5** (50% probability level). The molecule is located on a crystallographic C_2 axis. Averaged values are given for the distances involving the disordered DME ligand.

Table 5. Selected Distances (Å) and Angles (deg) for **5**

C1–C2	1.398(3)	C1–C3	1.389(3)
C3–C4	1.379(3)	C1–C5	1.502(3)
C5–C6	1.353(4)	C5–N1	1.366(3)
N1–C7	1.422(3)	Li1–N1	1.904(5)
Li1–O1 _{av} ^a	1.86(2)	Li1–O2 _{av} ^a	2.02(3)
C1–C5–C6	118.1(2)	C6–C5–N1	129.3(3)
C1–C5–N1	112.6(2)		

^a Averaged values are given for the distances involving the disordered DME ligand.

1.934(5) Å and Li1–N2 = 1.964(5) Å), which are in the typical range for lithium amides.¹³ As a consequence of the latter reaction, we sought to deprotonate the ketimine functionality in **1** itself with a hard, nonnucleophilic base, i.e., an lithium amide (Scheme 1).

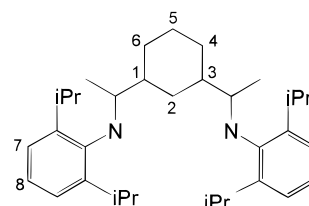
Indeed, reaction of **1** with 2 equiv of lithium dimethylamide, LiNMe₂, gave the corresponding diketiminate **5** (Scheme 1). The structure was immediately established from 1- and 2-D NMR spectroscopic data, with two doublets ($^2J = 2$ Hz) observed for the protons of the diastereotopic ketimine CH₂ groups in the ¹H NMR spectrum at 3.28 and 3.53 ppm being most diagnostically helpful. This assignment was unambiguously confirmed from the results of an X-ray crystal structure analysis, which is presented in Figure 5. The details of the data collection are given in Table 1; selected distances and angles are tabulated in Table 5.

The C–C and C–N distances (C5–C6 = 1.353(4) Å, C5–N1 = 1.366(3) Å) observed in the ketimine moiety as well as the short Li–N distance (Li–N1 = 1.904(5) Å) clearly suggested a pronounced amidic structure, i.e., CH₂=CN[–]-(2,6-C₆H₃(*i*-Pr)₂), quite similar to those observed by other groups, which have used such ligands with success for the complexation of a transition metal.¹⁴ On these grounds, it is deemed that introduction of the diimine ligand **1** into transition metal complexes via the

diketiminate **5** should be facile and is currently under investigation in our laboratories.

Experimental Section

Reactions were carried out under a dinitrogen atmosphere with thoroughly dried and N₂-saturated solvents using glovebox and Schlenk techniques. 1,3-Diacetylbenzene, 2,6-diisopropylaniline, and *n*-butyllithium and *tert*-butyllithium (1.6 and 1.5 M solutions in hexane, respectively) were purchased from Aldrich and used as received. ¹H, ¹³C, and ⁷Li NMR spectra were recorded on Varian Gemini 200 and 300 and Bruker Avance-500 spectrometers at 298 K. Chemical shifts are given in ppm and are referenced to the residual solvent shifts for ¹H and ¹³C NMR and to LiClO₄ for ⁷Li. The assignment of ¹H NMR and ¹³C NMR resonances is based on DEPT and two-dimensional ¹H–¹H COSY, ¹³C–¹H HSQC, and HMBC experiments. The numbering scheme applied is



IR spectra were measured on a Biorad FTS-45 Fourier IR spectrometer. X-ray crystal structure analyses were performed on a Stoe IPDS image plate system with a graphite-monochromated Mo K α (0.707 13 Å) beam. CHN analyses were carried out with a LECO CHNS-932 elemental analyzer at our institute. Cyclic voltammetry experiments were carried out in a glovebox in thoroughly purified THF with TBAPF₆ (0.3 M) as supporting electrolyte. Glassy-carbon working (1.2 mm diameter) and Ag/Ag⁺ reference electrodes were utilized with the potential being controlled by a BAS 100 W potentiostat. Ferrocene was added at the end of the measurement and the potential referenced to the Cp₂Fe/Cp₂Fe⁺ redox couple. GC/MS analyses were performed with a Hewlett-Packard 5890 Series II spectrometer, with the butane gas transferred/collected by standard high-vacuum manometry. Geometry optimizations at the UHF level on the radical anion 1,3-(–CH=NH)₂C₆H₄[–] and time-dependent calculations were carried out with the Turbomole program package and using a TZVP basis for all atoms.¹¹ The DFT calculation and Hirshfeld charge analysis on the model compound for **3**, 1,3,2-(–CH=NH)₂(Bu)C₆H₄[–], has been performed with DMOL applying dnp basis sets.¹² Both programs were used in their parallelized MPI versions installed on our 16-CPU parallel Linux cluster.

Synthesis of 1. To a solution of 6.75 g (38.1 mmol) of 2,6-diisopropylaniline and 2.81 g (17.3 mmol) of 1,3-diacetylbenzene in 75 mL of methanol was added 5 drops of formic acid, and the solution was stirred for 10 days at room temperature. The resulting solid was collected by filtration and washed with three 20 mL portions of cold methanol and two 20 mL portions of hexane. After recrystallization from hexane, the product was collected by filtration, washed with a small amount of MeOH, and finally dried under high vacuum to give compound **1** as an analytically pure pale yellow crystalline solid in 35% yield (2.91 g, 6 mmol). The monoimine could be recovered from the washing solutions and converted further to the diimine **1** as described above, giving a total yield of 54% (based on 1,3-diacetylbenzene). ¹H NMR (C₆D₆): δ 1.12 (d, $^3J = 7$ Hz, 12 H, CH(CH₃)₂); 1.17 (d, $^3J = 7$ Hz, 12 H, CH(CH₃)₂); 1.89 (s, 6 H, –N=CCH₃); 2.88 (sept, $^3J = 7$ Hz, 4 H, CH(CH₃)₂); 7.10–7.21 (m, 6 H, *o,o'*-(*i*-Pr)₂C₆H₃); 7.25 (t, $^3J = 8$ Hz, 1 H, CH(5)); 8.11 (dd, $^3J = 8$ Hz, $^4J = 2$ Hz, 2 H, CH(4,6)); 8.99 (s, 1 H, CH(2)). ¹³C{¹H} NMR (C₆D₆): δ 18.1 (N=CCH₃); 23.4 (CH(CH₃)₂); 23.8

(14) (a) Caro, C. F.; Hitchcock, P. B.; Lappert, M. F. *Chem. Commun.* **1999**, 1433. (b) Qian, B.; Scanlon, W. J., IV; Smith, M. R., III; Motry, D. H. *Organometallics* **1999**, *18*, 1693. (c) Lee, L. W. M.; Piers, W. E.; Elsegood, M. R. J.; Clegg, W.; Parvez, M. *Organometallics* **1999**, *18*, 2947 and references therein.

(CH(CH₃)₂); 29.2 (CH(CH₃)₂); 123.4 (CH(7 or 8)); 126.3 (C(2)); 128.3 (CH(7 or 8)); 128.8 (C(5)); 129.4 (C(4,6)); 136.1 (C_{ipso}-*i*-Pr); 139.5 (C(1, 3)); 147.2 (C_{ipso}-N); 164.8 (-N=CCH₃). IR (in hexane): 1641 (C=N); Anal. Calcd for C₃₄H₄₄N₂: C, 84.95; H, 9.23; N, 5.83. Found: C, 84.84; H, 9.37; N, 5.78. Single crystals suitable for X-ray diffraction were obtained by slow cooling of a saturated hexane solution.

Synthesis of the *n*-Bu Adduct 3. To a suspension of 981 mg (2.04 mmol) of the diimine **1** in 40 mL of dry diethyl ether was added an equimolar mixture of 1.27 mL of *n*-butyllithium (1.6 M in hexane) and 0.30 mL of TMEDA in 5 mL of pentane dropwise at room temperature, giving an ink blue solution. After the mixture was stirred for 21 h at room temperature, it was reduced under vacuum to half its original volume and then allowed to crystallize at -35 °C. Yield: 679 mg of **3**, red needles (50%). ¹H NMR (C₆D₆, room temperature): δ 1.02 (t, ³J = 7 Hz, 3 H, CH₃CH₂CH₂CH₂); 1.24 (d, ³J = 7 Hz, 6 H, CH(CH₃)₂); 1.30 (d, ³J = 7 Hz, 18 H, CH(CH₃)₂); 1.48 (m, 2 H, CH₃CH₂CH₂CH₂); 1.62 (broad s, 4 H, CH₂, TMEDA); 1.82 (broad s, 14 H, CH₃CH₂CH₂CH₂ and CH₃, TMEDA); 1.93 (m, 2 H, CH₃CH₂CH₂CH₂); 1.97 (s, 6 H, -N=CCCH₃); 3.15 (broad m, 4 H, CH(CH₃)₂); 4.99 (t, ³J = 7 Hz, 1 H, CH(2)); 5.38 (t, ³J = 7 Hz, 1 H, CH(5)); 6.86 (d, ³J = 7 Hz, 2 H, CH(4,6)); 7.20–7.23 (m, 6 H, *o,o'*-(*i*-Pr)₂C₆H₃). ¹³C{¹H} NMR (C₆D₆, room temperature): δ 14.9 (CH₃CH₂CH₂CH₂); 18.1 (CH₃CH₂CH₂CH₂); 23.0 (CH(CH₃)₂); 24.1 (CH(CH₃)₂); 24.5 (CH₃CH₂CH₂CH₂); 28.3 (CH(CH₃)₂); 29.0 (CH₃CH₂CH₂CH₂); 34.6 (C(2)); 35.0 (CNCH₃); 45.1 (CH₃, TMEDA); 56.3 (CH₂, TMEDA); 105.4 (C(5)); 118.1 (C(1)); 123.1 (CH_{arom}); 123.3 (CH_{arom}); 127.8 (C(4,6)); 139.2 (C_{ipso}-*i*-Pr); 149.9 (C_{ipso}-N); 165.1 (C=N). ⁷Li NMR (C₆D₆, room temperature): δ 0.06 (s). Anal. Calcd for C₄₄H₆₉LiN₄: C, 79.95; H, 10.52; N, 8.48. Found: C, 79.79; H, 10.41; N, 8.67. Single crystals suitable for X-ray diffraction were obtained by crystallization in pentane at -35 °C.

Synthesis of the Di-*t*-Bu Adduct 4. To a well-stirred suspension of the diimine **1** (215 mg, 0.45 mmol) in 0.60 mL of pentane was added 2 equiv (0.90 mmol) of *tert*-butyllithium (1.5 M in hexane) dropwise. A deep red solution was obtained, which was stirred for 17 h and then cooled to -35 °C, from which **4** was obtained as yellow-orange crystals (92 mg, 135 μmol). Yield: 30%. ¹H NMR (C₆D₆, room temperature): δ 0.62 (d, ³J = 7 Hz, 3 H, CH(CH₃)₂); 0.94 (t, ³J = 7 Hz, Et₂O); 1.10 (d, ³J = 7 Hz, 3 H, CH(CH₃)₂); 1.17 (d, ³J = 7 Hz, 3 H, CH(CH₃)₂); 1.23 (d, ³J = 7 Hz, 3 H, CH(CH₃)₂); 1.25 (d, ³J = 7 Hz, 3 H, CH(CH₃)₂); 1.25 (d, ³J = 7 Hz, 3 H, CH(CH₃)₂); 1.30 (broad s, 9 H, C(CH₃)₃ at C(4)); 1.37 (d, ³J = 7 Hz, 3 H, CH(CH₃)₂); 1.50 (s, 9 H, C(CH₃)₃ at C(2)); 1.52 (d, ³J = 7 Hz, 3 H, CH(CH₃)₂); 1.94 (s, 3 H, N=CCH₃); 1.97 (s, 3 H, N=CCH₃); 2.42 (sept, ³J = 7 Hz, 1 H, CH(CH₃)₂); 3.17 (q, ³J = 7 Hz, Et₂O); 3.32 (sept, ³J = 7 Hz, 1 H, CH(CH₃)₂); 3.55 (sept, ³J = 7 Hz, 1 H, CH(CH₃)₂); 3.66 (broad s, 1 H, CH(4)); 3.79 (sept, ³J = 7 Hz, 1 H, CH(CH₃)₂); 4.22 (s, 1 H, CH(2)); 5.28 (dd, ³J = 9 Hz, ³J = 2 Hz, 1 H, CH(5)); 6.48 (d, ³J = 9 Hz, 1 H, CH(6)); 6.99–7.30 (m, 6 H, *o,o'*-(*i*-Pr)₂C₆H₃). ¹³C{¹H} NMR (C₆D₆): δ 14.3 (Et₂O); 16.8 (N-CCH₃); 21.2 (CH(CH₃)₂); 22.1 (CH(CH₃)₂); 22.8 (CH(CH₃)₂); 23.6 (CH(CH₃)₂); 24.1 (CH(CH₃)₂); 25.0 (C(CH₃)₃ at C(4)); 25.4 (CH(CH₃)₂); 25.8 (CH(CH₃)₂); 26.2 (CH(CH₃)₂); 27.2 (CH(CH₃)₂); 27.3 (CH(CH₃)₂); 27.6 (CH(CH₃)₂); 29.3 (CH(CH₃)₂); 30.0 (C(CH₃)₃ at C(2)); 32.7 (C(CH₃)₃ at C(4)); 38.7 (C(CH₃)₃ at C(2)); 52.7 (C(2)); 65.2 (Et₂O); 68.8 (C(4)); 94.2 (C(1) or C(3)); 114.0 (C(1) or C(3)); 118.8 (C(5)); 119.0 (CH_{arom}); 121.5 (CH_{arom}); 121.5 (CH_{arom}); 123.3 (CH_{arom}); 124.1 (CH_{arom}); 124.8 (CH_{arom}); 128.8 (C(6)); 137.6 (C_{ipso}-*i*-Pr); 138.1 (C=N); 140.5 (C_{ipso}-*i*-Pr); 142.7 (C_{ipso}-*i*-Pr); 145.3 (C_{ipso}-*i*-Pr); 148.7 (C_{ipso}-N); 148.9 (C_{ipso}-N); 156.3 (C=N). The ¹³C NMR resonances of carbon atoms C(1) and C(3) could not be unambiguously assigned due to missing signals in the HSQC and HMBC experiments. ⁷Li NMR (C₆D₆, room temperature): δ -1.77 (s); 1.60 (broad s). Attempts to obtain correct elemental analysis data have so far been unsuccessful. Single crystals suitable

for X-ray diffraction were obtained by crystallization in pentane with some ether added at -35 °C.

Synthesis of the Diketimate 5. (a) Deprotonation of **1 with LiNMe₂.** To a suspension of 110 mg (2.15 mmol) of LiNMe₂ in 10 mL of dry diethyl ether was added a solution of the diimine **1** (258 mg, 0.54 mmol) in 0.2 mL of DME at room temperature. The obtained suspension was stirred for 20 h, reduced in vacuo, and finally dissolved in toluene. After filtration through a sintered-glass frit, the volume of the solution was reduced under high vacuum and recrystallized, with a small amount of DME added, at -35 °C. Yield: 103 mg (28%).

(b) Deprotonation with *n*-BuLi/TMEDA. To a solution of 300 mg (624 μmol) of diimine **1** in 15 mL of diethyl ether and 3 mL of TMEDA was added a solution of 0.78 mL (1.25 mmol) of *n*-BuLi (1.6 M in hexane) in 3 mL of TMEDA dropwise. After the mixture was stirred for 1 h at room temperature, the solid was collected by filtration, washed with pentane, and dried under high vacuum. From recrystallization in DME at -35 °C, the diketimate **5** was obtained as pale yellow plates in 46% yield (192 mg, 285 μmol). ¹H NMR (C₆D₆, room temperature): δ 1.38 (d, ³J = 7 Hz, 12 H, CH(CH₃)₂); 1.62 (d, ³J = 7 Hz, 12 H, CH(CH₃)₂); 2.56 (s, 12 H, CH₃, DME); 2.59 (s, 8 H, CH₂, DME); 3.28 (d, ²J = 2 Hz, 2 H, -NC=CH₂); 3.53 (d, ²J = 2 Hz, 2 H, -NC=CH₂); 3.91 (sept, ³J = 7 Hz, 4 H, CH(CH₃)₂); 7.19 (t, ³J = 7 Hz, 1 H, CH(5)); 7.26 (t, ³J = 7 Hz, 2 H, CH(8)); 7.44 (d, ³J = 7 Hz, 4 H, CH(7)); 7.90 (d, ³J = 7 Hz, 2 H, CH(4,6)); 8.40 (s, 1 H, CH(2)). ¹³C{¹H} NMR (C₆D₆): δ 25.2 (CH(CH₃)₂); 25.3 (CH(CH₃)₂); 28.1 (CH(CH₃)₂); 58.8 (CH₂, DME); 69.0 (-NC=CH₂); 69.8 (CH₃, DME); 121.5 (C(8)); 122.0 (C(2)); 123.2 (C(7)); 126.5 (C(4,6)); 128.9 (C(5)); 144.5 (C_{ipso}-*i*-Pr); 150.5 (C(1,3)); 152.7 (C_{ipso}-N); 162.0 (-NC=CH₂). ⁷Li NMR (C₆D₆, room temperature): δ 0.26 (s). Anal. Calcd for C₄₂H₆₂Li₂N₂O₄: C, 74.97; H, 9.29; N, 4.16. Found: C, 74.71; H, 9.19; N, 4.42. Single crystals suitable for X-ray diffraction were obtained at room temperature by slow diffusion of pentane into a solution of **5** in DME.

X-ray Crystal Structure Analyses. General Remarks. Suitable single crystals were mounted on glass fibers in polyisobutylene oil (Aldrich, 38896-6), transferred on the goniometer head to the diffractometer, and cooled to -80 or -90 °C in a N₂ cryostream. The data sets were collected with graphite-monochromated Mo Kα radiation (0.707 13 Å) on a Stoe IPDS image plate diffractometer. Intensities were corrected for Lorentz and polarization effects. The structures were solved using direct methods with the SHELXS-86 program package.¹⁵ The refinements were carried out with SHELXL-93 using all unique *F*_o² values.¹⁶ Unless otherwise specified, all non-hydrogen atoms were treated anisotropically with the positions of the hydrogen atoms calculated in idealized positions (C-H bonds fixed at 0.96 Å) and refined as a riding model. The details of the data collections and refinements, including *R* values, are summarized in Table 1.

Compound 1. Several crystals were checked, which all appeared to be at least partially twinned, which led to problems with the space group determination. Possible space groups were *Cc*, *C2c*, and *Fdd2*, respectively. The structure was finally solved and refined in spacegroup *Fdd2* (No. 43) with a twin refinement (TWIN card). The molecule is located on a crystallographic C₂ axis passing through atoms C2 and C4.

Compound 3. The hydrogen atoms H2, H4, H5, and H6 of the central ring were located in the difference Fourier map and were refined isotropically.

Compound 4-0.5Et₂O. The hydrogen atoms H2, H4, H5, and H6 of the central ring were located in the difference

(15) Sheldrick, G. M. SHELXTL PLUS; University of Göttingen, Göttingen, Germany, 1988.

(16) Sheldrick, G. M. SHELXL 93; University of Göttingen, Göttingen, Germany, 1993.

Fourier map and were refined isotropically. A second ether molecule (C47, C48, C49, C50, O2) located in the unit cell was disordered and was refined isotropically with identical thermal displacement parameters for the carbon atoms (EADP cards for C47–C50) and applied constraints for the C–O and C–C distances (DFIX 1.45 for C48–O2 and C49–O2 and DFIX 1.54 for C47–C48 and C49–C50).

Compound 5. The molecule is located on a crystallographic C_2 axis passing through atoms C2, C4, H2, and H4. Hydrogen atoms H2 and H6A, H6B were located in the difference Fourier map and were refined isotropically. The isopropyl groups were disordered and were refined with split positions for the methyl groups C14, C15 and C17, C18 and converged at occupation factors of 0.67/0.33 (C14, C15) and 0.56/0.44 (C17, C18). In addition, the DME ligand (C19–C22 and O1, O2) was found

to be disordered and was refined with two split positions, which converged at occupation factors of 0.69 and 0.31.

Acknowledgment. We are indebted to Prof. Heinz Berke for his generous support. We thank Dr. Thomas Fox for assistance with the NMR measurements.

Supporting Information Available: ^1H NMR spectrum of compound **4** and tables of atomic coordinates and equivalent isotropic displacement coefficients, anisotropic thermal parameters, bond distances and angles, and contact distances and Ortep plots for **1**, **3**, **4**·0.5Et₂O, and **5**. This material is available free of charge via the Internet at <http://pubs.acs.org>.

OM000084K